Proceedings of the ASME 2016 Fluids Engineering Division Summer Meeting
FEDSM2016
July 10-14, 2016, Washington, DC, USA

FEDSM2016-7597

# LAMINAR-TURBULENT TRANSITION FLOWS OF NON-NEWTONIAN SLURRIES: MODELS ASSESSMENT

**Kofi Freeman K. Adane***
Alberta Innovates-Technology Futures
Devon, Alberta, Canada

**Martin Agelin-Chaab**
University of Ontario Institute of Technology
Oshawa, Ontario, Canada

## ABSTRACT

In this study a qualitative assessment of transitional velocity engineering models for predicting non-Newtonian slurry flows in a horizontal pipe was performed using data from wide pipe diameters (25 - 268 mm). In addition, Gamma Theta transition model was used to compute selected flow conditions. In general, it was observed that most of the current engineering models predict conservative transitional velocities. However, caution should be exercised in design situations where both pipe diameter and viscoplastic viscosity influence the value of Hedström number. It was found that the Gamma Theta transition model predicted a laminar flow condition in the fully developed region which is contrary to what has been observed in experiment.

## INTRODUCTION

Non-Newtonian slurry flows are found in many industries, especially in the mining and petrochemical industries. Also, sludge from municipal waste treatment systems usually behave as non-Newtonian fluids. Driven by regulatory requirements, and cost savings or design constraints, these slurries tend to have high solid content. The slurries of interest here are those that contain fine solids such that the mixture can be considered a "continuum" or normally referred to as homogeneous or non-settling slurries in the industries. Thus, settling slurries or slurry containing medium to coarse solids are not considered in this study although they might share the same fluid characteristics.

Non-Newtonian slurries usually have a yield stress and consequently behave as viscoplastic fluids (see works by Xu *et al* [1], Slatter and Wasp [2], Wilson and Thomas [3], and van den Heever [4]). Because of the yield stress and its accompanying high viscosity, these slurries are normally transported in laminar flow conditions. Turbulent flow conditions of these slurries are also possible but will be subjected to relatively high pumping cost and piping pressure rating. Because of the advantages of laminar flow conditions such as low pumping cost and piping wear, several models have been developed to predict the onset of turbulence or transition velocity. These engineering models helped the designer to optimize the hydraulic system for the slurry transport. The other indirect benefit of these models is that they are used to scale-up from small to large pipe diameters.

Most of the transition velocity models are either empirical or semi-empirical, and as a result their use for scale-up might not necessarily achieve accurate results. In this paper, a selection of engineering models is used to predict transition velocity for previously reported experimental data. In addition, the Menter Transition Model is adopted to solve the flow field of non-Newtonian slurry at or near the transition velocity. It is worth mentioning that the intent of this work is not to argue for or against particular model but to contribute to the ongoing research on this subject. Furthermore, the Menter Transition Model is a semi-empirical model that is calibrated for aerodynamics, and an attempt of using it is not for verification or validation but rather to provide some basis for further development for broad industrial applications. The authors are not aware of any similar work in the open literature.

## TRANSITIONAL VELOCITY MODELS

Unlike Newtonian fluids where viscosity is constant for a given flow condition, the viscosity of non-Newtonian fluids varies. In this study, only shear-rate and yield fluids, the so-called viscoplastic fluids are considered. These fluids will not move until the applied shear stress, $\tau$ is higher than the fluid yield stress, $\tau_y$. It has been observed that most non-Newtonian slurries of interest here tend to have such behavior (see works by Xu *et al* [1], Slatter and Wasp [2], Wilson and Thomas [3], van den Heever [4], Malin [5], Guzel *et al* [6], and Sutherland *et al* [7]) and can be defined by:

$$\tau = \tau_y + \mu_p \gamma \quad \text{or} \quad \mu = \mu_p + (\tau_y/\gamma) \tag{1}$$

*corresponding author

where $\mu_p$ is the fluid plastic viscosity, $\mu$ is the apparent viscosity and ¥ is the shear-rate. It is worth mentioning that, both Casson, Herschel-Bulkley and other non-Newtonian models have also been used to describe non-Newtonian slurries, but only Bingham fluids defined in Eqn. (1) will be considered in the present work.

Similar to Newtonian flows in pipes, several works have shown that the transitional flow conditions also occur at a range of flow velocities for any given fluid property and pipe geometry [2-6]. Although, several definitions have been used for Reynolds number, *Re*, the agreement among previous works is the definition based on pipe inner diameter, *D*, velocity, *U*, fluid plastic viscosity, $\mu_p$ and density, ° (*Re* = °*UD*/$\mu_p$). In addition, the onset of the transition flow condition also occurs at *Re* = 2100.

In the literature, several models have been proposed or used to predict transitional velocity in the horizontal non-Newtonian slurry flows, notably, Slatter and Wasp [2], Wilson and Thomas [3], Lui et al [8], and Swamee and Aggarwal [9]. Full details of these and other models will be provided subsequently.

*Slatter and Wasp (SW) [2]:*

$$V_T = \begin{cases} 26\left(\frac{\tau_y}{\rho}\right)^{0.5} & He \geq 1.5\times10^5 \\ 155\frac{\tau_y{}^{0.35}}{\rho^{0.65}}\left(\frac{\mu_p}{D}\right)^{0.3} & 1700 < He < 1.5\times10^5 \\ \frac{2100\mu_p}{\rho D} & He \leq 1700 \end{cases} \quad (2)$$

*Wilson and Thomas (WT) [3]:*

$$V_T = \begin{cases} 25\left(\frac{\tau_y}{\rho}\right)^{0.5} & He \geq 10^5 \\ \frac{80\mu_p}{\rho D}He^{0.4} & 1700 < He < 10^5 \\ \frac{2100\mu_p}{\rho D[1.0+8.3\times10^{-8}(\log_{10}He)^{13}]} & He \leq 1700 \end{cases} \quad (3)$$

*Lui et al (Lui) [8]:*

$$V_T = 0.4 + 22.1(\tau_y/\rho)^{0.5} \quad (4)$$

*Swamee and Aggarwal (SA) [9]:*

$$V_T = \begin{cases} 161\frac{\tau_y{}^{0.35}}{\rho^{0.65}}\left(\frac{\mu_p}{D}\right)^{0.3} & 10^8 < He \leq 10^{12} \\ \frac{2100\mu_p}{\rho D}\left[1+\frac{He}{3600}\right]^{0.35} & 1 \leq He \leq 10^8 \end{cases} \quad (5)$$

where $V_T$ is the transitional velocity and *He* is the Hedström number (= ²$_y$ ° $D^2/\mu_p{}^2$). With the exception of Lui et al [8], all the other three models use *Re* = °*UD*/$\mu_p$. It should also be remarked that there are several other transitional velocity models in the literature but only most commonly applied and those with the potential for industrial applications due to their simplicity are the focus of the present study.

Another approach that has been used in the literature which WT model is somewhat based on is the Hedström intersection method [10] (see Fig. 1). Hedström postulated that transition occurs at the intersection of the laminar and turbulent friction factor curves. However, the major drawback of this method is that unlike laminar flow condition, there is no analytical solution for turbulent flow conditions. Therefore one has to completely rely on a model. Thus, the accuracy of this method depends on the model used for the turbulent flow condition. In addition, as it can be seen in Fig. 1, its success will depend highly on an abrupt increase of head loss at the laminar-turbulent transition, and flows with absence of this abrupt will be a challenge [11].

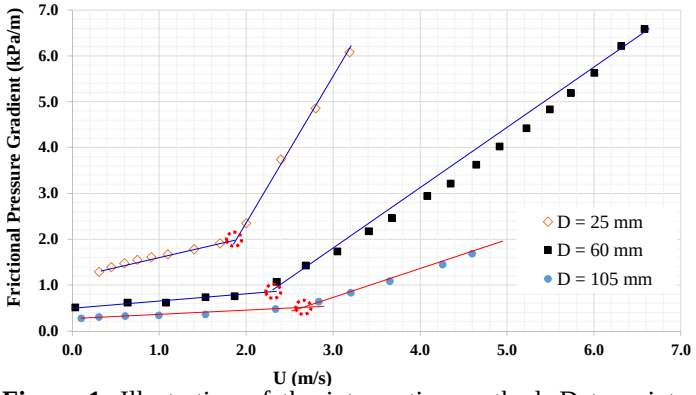


**Figure 1**: Illustration of the intersection method. Data points from Wilson and Thomas [3].

## NUMERICAL PROCEDURE

***Governing Equations:***

In addition to transitional velocity models stated in the previous section, various flow conditions are numerically solved. The governing equations are:

$$\nabla \bullet \vec{u} = 0 \quad (6)$$

$$\rho\left(\frac{\partial \vec{u}}{\partial t}+\vec{u}\bullet\nabla\vec{u}\right)=-\nabla p+\nabla\bullet\left(\mu\left(\nabla\vec{u}+(\nabla\vec{u})^{T}\right)\right)-\nabla R \tag{7}$$

where $\vec{u}$ is the velocity vector, $\rho$ is the density, $p$ is the total pressure which is the sum of dynamic and static components, and $R$ is Reynolds stresses. The shear stress transport (SST) turbulent model [12] is adopted to compute the Reynolds stress term, $R$ (see Eqn. 7).

$$R=\rho\overline{u_i u_j}\cong\frac{2}{3}\rho k-\mu_t\left(\frac{\partial \vec{u}_i}{\partial x_j}+\frac{\partial \vec{u}_j}{\partial x_i}\right) \tag{8}$$

where $k$ is turbulent kinetic energy and $\mu_t$ denotes eddy or turbulent viscosity. The equations solved for SST model are given as:

$$\rho\left(\frac{\partial k}{\partial t}+\frac{\partial(\vec{u}k)}{\partial x_i}\right)=\frac{\partial}{\partial x_i}\left(\left(\mu+\frac{\mu_t}{\sigma_{k1}}\right)\frac{\partial k}{\partial x_i}\right)+(P_k-\beta\rho k\omega) \tag{9}$$

$$\rho\left(\frac{\partial \omega}{\partial t}+\frac{\partial(\vec{u}\omega)}{\partial x_i}\right)=\frac{\partial}{\partial x_i}\left(\left(\mu+\frac{\mu_t}{\sigma_{\omega 1}}\right)\frac{\partial \omega}{\partial x_i}\right)+\alpha\frac{\omega}{k}P_k-\beta\rho\omega^2+2(1-F)\rho\frac{\sigma_{\omega 2}}{\omega}\frac{\partial k}{\partial x_i}\frac{\partial \omega}{\partial x_i} \tag{10}$$

The eddy viscosity is given as: $\mu_t=\dfrac{\alpha\rho k}{\max(\alpha\omega,\Omega F_1)}$

where specific dissipation rate, $\omega = \varepsilon/k$, $\sigma_{k1}$, $\sigma_{\omega 1}$, $\sigma_{\omega 2}$, $\beta$, $\beta_1$ and $\gamma$ are constants with values 2.0, 2.0, 0.856, 0.09, 0.0828 and 5/9, respectively, $\Omega$ is the invariant measure of the strain rate, and the blending factors ($F$ and $F_1$) are given as:

$$F=\tanh(\Phi^4);\quad \Phi=\min\left(\max\left(\frac{\sqrt{k}}{\beta\omega y},\frac{500\nu}{y^2\omega}\right),\frac{4\rho k\sigma_{\omega 2}}{CD_{k\omega}y^2}\right) \tag{11}$$

$$CD_{k\omega}=\max\left(\frac{2\rho\sigma_{\omega 2}}{\omega}\frac{\partial k}{\partial x_i}\frac{\partial \omega}{\partial x_i},1.0\times10^{-10}\right) \tag{12}$$

$$F_1=\tanh(\Phi_1^2);\quad \Phi_1=\max\left(\frac{2\sqrt{k}}{\beta\omega y},\frac{500\nu}{y^2\omega}\right) \tag{13}$$

The eddy viscosity in Eqn. (10) is based on the definition used in the Wilcox $k$-$\omega$ model [13] which is given as $\mu_t = \rho\, k / \omega$. It should be noted that in the present study, the effect of buoyancy forces on turbulence is ignored, and therefore expressions accounting for these forces are not included in the turbulence model equation given here.

***Transition Model:***

The Gamma Theta Model (GTM) for transition flows is adopted for the present work. Here, only a brief note applicable to the present work is given but more details can be found in works by Menter and co-authors [14-16]. For this model, in addition to the blending function, the production and destruction terms in $k$-equation (see Eqn. 9) were only modified to the following:

$$\tilde{P}_k=\gamma P_k;\quad \tilde{D}_k=\min(\max(\gamma,0.1),1.0)(\rho k\omega)$$

$$R_y=\frac{\rho y\sqrt{k}}{\mu};\quad F_3=e^{-(R_y/120)^8};\ \tilde{F}_1=\max(F_1,F_3)$$

The Gamma Theta Model is based on two transport equations: the intermittency, $\gamma$ and transition onset criteria in terms of momentum thickness Reynolds number, $Re_{\theta t}$ which are given in Eqns. 14 and 15, respectively.

$$\frac{\partial(\rho\gamma)}{\partial t}+\frac{\partial(\rho\vec{u}\gamma)}{\partial x_i}=S_\gamma+\frac{\partial}{\partial x_i}\left[\left(\mu+\frac{\mu_t}{\sigma_f}\right)\frac{\partial\gamma}{\partial x_i}\right] \tag{14}$$

$$\frac{\partial(\rho\tilde{\mathrm{Re}}_{\theta t})}{\partial t}+\frac{\partial(\rho\vec{u}\tilde{\mathrm{Re}}_{\theta t})}{\partial x_i}=S_{\theta t}+\frac{\partial}{\partial x_i}\left[2\left(\mu+\frac{\mu_t}{\sigma_{\theta t}}\right)\frac{\partial\tilde{\mathrm{Re}}_{\theta t}}{\partial x_i}\right] \tag{15}$$

$$S_\gamma=f\left(F_{length},\mathrm{Re}_{\theta c},\gamma,\ldots\right)$$

$$S_{\theta t}=6.0\times10^{-5}\rho^2u^2\left(\mathrm{Re}_{\theta t}-\tilde{\mathrm{Re}}_{\theta t}\right)\left(1.0-F_{\theta t}\right)$$

where $S_\gamma$ and $S_{\theta t}$ are source terms for respective transport equation. For Gamma Theta Model, a shear-rate Reynolds number ($Re_v = \rho\, y_n^2\, \Omega\, /\, \mu$, where $y_n$ is the distance from the nearest wall, $\Omega$ is the absolute value of the strain rate) is use to trigger the onset of transition instead of momentum thickness Reynolds number [14-16]. Although, both transport equations depend on the local flow parameters they contain three empirical parameters: $F_{length}$ which is the length of the transition zone, $Re_{\theta c}$ is the critical Reynolds number which is the point where the model is activated in order to match both $Re_{\theta t}$ and $F_{length}$, and $Re_{\theta t}$ which is a function of turbulence intensity and Thwaites' pressure gradient coefficient (see [14-16]). Even though the relationships among these parameters are proprietary, they were obtained using Newtonian fluids. It is not clear if they will hold for non-Newtonian fluids. It is also worth noting that, the turbulence intermittency, $\gamma$ is enforced to a value of 0.02 for relaminarization.

***Numerical Solution:***

The general numerical solution procedure is the same as those given in detailed elsewhere by one of the authors [17-19] and will not be repeated here. A uniform velocity was specified at the inlet whereas a zero pressure was specified at the outlet. A no-slip boundary condition was specified at the walls. The GTM in ANSYS CFX was used for the present work. Computations with various turbulent intensity values at inlet for kinetic energy were also performed. It was observed that specifying the turbulent intensity value has a significant influence on the turbulent kinetic energy values instead of other parameters such as turbulent intermittency, pressure drop, et cetera. However, since no experimental information is available, it was decided to use zero gradient for both turbulent kinetic energy, $k$ and specific dissipation rate, $\omega$ at inlet.

Also, the solution procedure assumed a boundary condition for $\gamma$ at the wall as zero normal flux and 1.0 at the inlet. Meanwhile, for $\tilde{R}e_{\theta t}$ at the wall, a zero flux was used whereas at the inlet it was empirically calculated using the inlet turbulence

intensity. In addition, in order to capture the laminar and transitional boundary layers correctly, all grids used have $y^+$ less than 1.0.

## DISCUSION

There are several experimental data in the literature and most of them are collected from pipe flow loops. However, only selected (see Table 1) of those previously published data will be used for evaluation in the present work. These previous studies were selected based on the following assumptions:

1. Only fluids or data that have no elastic effects. Therefore, all high molecular weight polymers based viscoplastic fluids (e.g. Carbopol) are excluded.
2. Only Bingham or Casson viscoplastic fluids are considered since Herschel-Bulkley fluids do not become Newtonian fluid at high shear rate.
3. Authors gave sufficient background information to assess their quality.
4. With exception of Wilson and Thomas [3] data on 105 mm, none of the authors of the models have used any data for evaluation.

In situations where previous authors do not provide the rheological data for the fluid, fitting was done to the laminar data to determine those parameters based on observed reported model fitting. In addition, those data in Table 1 were selected to cover a wide range of pipe diameters and Hedström numbers. It should also be mentioned that it is assumed that the fluid rheology does not change under the turbulent flow conditions.

In Table 1, the experimental data for $V_T$ was obtained by taking the last laminar data points in the experimental data sets. The laminar data are determined by comparing experimental data with analytical results assuming ±10% error. While this error value is somewhat arbitrary since most authors did not report the experimental uncertainties, it is a reasonable value. Although, a similar method has been used by van den Heever and co-workers [4, 7], it is not clear if they used analytical results to determine the last laminar value. Also, where available respective fluid properties are included in Table 1.

It is evident in Table 1 that the performance of the models is not the same. Swamee and Aggarwal (SA) consistently under-predicted the transition velocities whereas Wilson and Thomas (WT) seems to give reasonable prediction. Because there is limited data from large pipe diameters (> 105 mm or 4 inches), caution should be exercised in extrapolating their performance. It was observed from Table 1 that, generally the models with exception of SA over-predicted the transition velocities.

The models also are sensitive to fluid yield stress and pipe diameter. For the same fluid, increasing the pipe diameter tends to exacerbate the percentage error. With the exception of Lui model, all the models used Hedström number as criteria with separate expression for different range of *He* values. The main issue is that, this dimensionless parameter is the square of pipe diameter and that can push its value to next range thereby overestimating the transition velocities (see Eqns. 2-5). Xu et al [1] and Litzenberger [20] reported that the method used to estimate the fluid model parameters has greater influence on viscoplastic viscosity than yield stress. A plot of the transition velocities and Hedström number, *He* for both experimental values and WT model results are presented in Fig. 2. It is clear from Fig. 2 that applicability of the model is limited to *He* less than 1.5 x $10^6$ for these datasets. Considering that for a specific fluid the error can increase from 6% to 20% by just changing pipe diameter from 60 mm to 80 mm despite the so-called large pipe diameter criteria has been met. Perhaps, the transition velocity is not simply a function of fluid yield stress and density at higher Hedström numbers.

Another interesting observation is the relative good performance of Lui in Fig. 3 and Table 1. In fact, unlike WT which is based on phenomenological approach of pressure gradient, Lui is purely empirical. From Table 1, the Lui model seems not applicable to relatively low yield stress, generally less than 8 Pa irrespective of pipe diameter. Also, for the same fluid, the error increases significantly with increasing pipe diameter for these yield stress values. While it might be simple to use, engineering accuracy might be compromised for its simplicity.

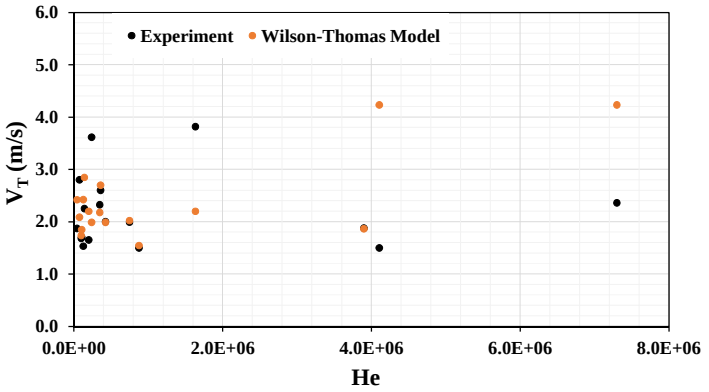


**Figure 2**: Transition velocity versus Hedström number

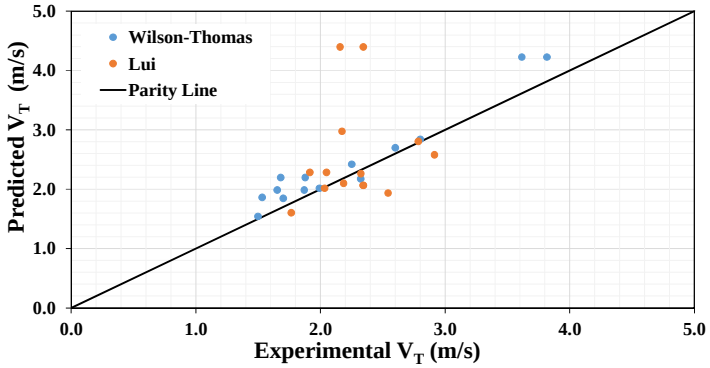


**Figure 3**: Parity plot of transition velocity from prediction and experiments

**Table 1:** Dataset from the literature

| Fluids | | | | | Author | | Expt. | WT | | SW | | SA | | Lui | |
|---|---|---|---|---|---|---|---|---|---|---|---|---|---|---|---|
| Composition | r (kg/m$^3$) | $\tau_y$(Pa) | $\mu_p$(Pa·s) | D (m) | | He | $V_T$(m/s) | $V_T$(m/s) | Error | $V_T$(m/s) | Error | $V_T$(m/s) | Error | $V_T$(m/s) | Error |
| Kaolinite pond sludge (oilsands tailings)* | 1598 | 12.1 | 0.0619 | 0.263 | Xu et al [1] | 3.5E+05 | 2.32 | 2.18 | -6.3% | 2.26 | -2.6% | 1.54 | -33.7% | 2.32 | 0.0% |
| Water+17% Kaolin | 1278 | 8.3 | 0.0189 | 0.158 | | 7.5E+05 | 1.99 | 2.02 | 1.4% | 2.10 | 5.5% | 1.27 | -36.1% | 2.19 | 9.7% |
| Water+14.8% Kaolin | 1228 | 4.7 | 0.0128 | 0.158 | | 8.8E+05 | 1.50 | 1.54 | 3.1% | 1.61 | 7.2% | 0.95 | -36.6% | 1.76 | 17.8% |
| Water+10% Kaolin | 1161 | 1.9 | 0.0015 | 0.026 | | 6.5E+05 | | 1.01 | | 1.05 | | 0.65 | | 1.29 | |
| Water+14% Kaolin | 1228 | 14.3 | 0.0057 | 0.026 | Litzenberger [20] | 3.6E+05 | 2.60 | 2.70 | 3.8% | 2.81 | 7.9% | 1.90 | -27.0% | 2.78 | 7.1% |
| Water+14% Kaolin+0.10%TSPP | 1228 | 4.4 | 0.0021 | 0.026 | | 8.2E+05 | | 1.50 | | 1.56 | | 0.93 | | 1.72 | |
| Water+14% Kaolin+0.13%TSPP | 1228 | 6.7 | 0.0072 | 0.026 | | 1.1E+05 | 1.70 | 1.85 | 8.6% | 2.02 | 18.7% | 1.58 | -7.3% | 2.03 | 19.6% |
| Water+14% Kaolin+0.27%TSPP+10g Dispersant | 1228 | 7.9 | 0.0092 | 0.026 | | 7.6E+04 | 2.00 | 2.08 | 4.2% | 2.30 | 15.1% | 1.80 | -9.8% | 2.17 | 8.6% |
| Water+14% Kaolin+0.27%TSPP+15g Dispersant | 1228 | 15.9 | 0.0096 | 0.026 | | 1.4E+05 | 2.80 | 2.84 | 1.6% | 2.98 | 6.4% | 2.32 | -17.3% | 2.91 | 4.1% |
| Water+17% Kaolin+0.13%TSPP | 1278 | 12.0 | 0.0090 | 0.026 | | 1.3E+05 | 2.25 | 2.42 | 7.7% | 2.58 | 14.6% | 2.01 | -10.7% | 2.54 | 13.0% |
| -* | 1350 | 7.5 | 0.0054 | 0.105 | Wilson & Thomas [4] | 3.9E+06 | 1.53 | 1.86 | 21.6% | 1.94 | 26.5% | 0.91 | -40.3% | 2.05 | 33.6% |
| Water+22.6% Kaolin+0.03%TSPP | 1384 | 6.5 | 0.0160 | 0.053 | Spelay [21] | 9.9E+04 | 1.50 | 1.74 | 15.8% | 1.89 | 26.2% | 1.48 | -1.4% | 1.91 | 27.7% |
| Water+6% Bentonite | 1100 | 8.5 | 0.0061 | 0.013 | Heever [6] | 4.3E+04 | 2.36 | 2.42 | 2.5% | 2.75 | 16.5% | 2.18 | -7.6% | 2.34 | -0.7% |
| | 1100 | 8.5 | 0.0061 | 0.028 | | 2.0E+05 | 1.88 | 2.20 | 17.1% | 2.29 | 21.7% | 1.69 | -9.7% | 2.34 | 24.8% |
| | 1100 | 8.5 | 0.0061 | 0.080 | | 1.6E+06 | 1.68 | 2.20 | 30.8% | 2.29 | 36.0% | 1.23 | -26.8% | 2.34 | 39.4% |
| Water+7.34% Bentonite | 1100 | 7.0 | 0.0107 | 0.060 | | 2.4E+05 | 1.87 | 1.99 | 6.3% | 2.07 | 10.6% | 1.49 | -20.2% | 2.16 | 15.4% |
| | 1100 | 7.0 | 0.0107 | 0.080 | | 4.2E+05 | 1.65 | 1.99 | 20.3% | 2.07 | 25.1% | 1.36 | -17.4% | 2.16 | 30.5% |
| | 1100 | 7.0 | 0.0107 | 0.150 | | 1.5E+06 | N/A | 1.99 | | 2.07 | | 1.13 | | 2.16 | |
| Water+9% Bentonite | 1150 | 32.9 | 0.0058 | 0.060 | | 4.1E+06 | 3.82 | 4.23 | 10.8% | 4.40 | 15.2% | 2.06 | -46.0% | 4.14 | 8.4% |
| | 1150 | 32.9 | 0.0058 | 0.080 | | 7.3E+06 | 3.61 | 4.23 | 17.0% | 4.40 | 21.7% | 1.89 | -47.7% | 4.14 | 14.5% |
| | 1150 | 32.9 | 0.0058 | 0.150 | | 2.6E+07 | N/A | 4.23 | | 4.40 | | 1.56 | | 4.14 | |
| *-property either assumed or determined from measurment data | | | | | | | | | | | | | | | |

***Gamma Theta Model (GTM):***

Numerical computation was only performed on selected works, Spelay [21] and Xu et al [1]. Figure 4 shows a typical velocity profiles for velocities around the predicted transition velocity in Table 1 for Xu et al [1]. The transition velocity is not discernable on the figure despite the fact that Peixinho et al [22] reported slight change in velocity profile shape at the transition onset. It is worth mentioning that, they used a Herschel-Bulkley viscoplastic fluid which is made from a high molecular weight polymer.

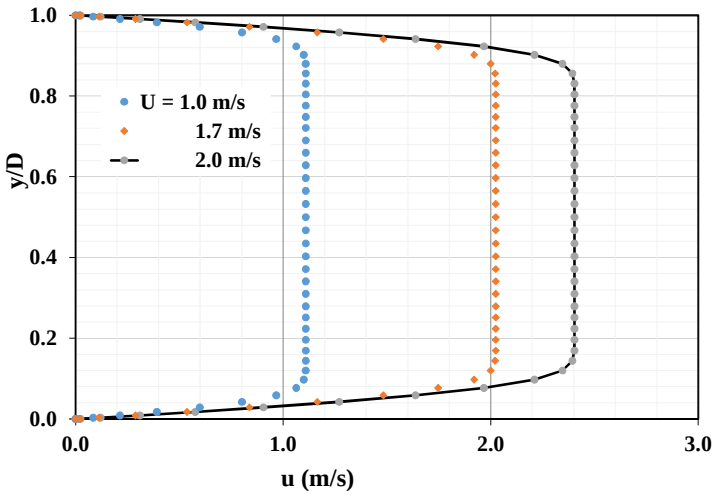


**Figure 4**: Prediction of the velocity profile using GTM at various bulk velocities, *U*.

The pressure drop from the laminar analytical values and the present work are compared with those from Spelay [21] and Xu et al [1] in Figs. 5 and 6, respectively. The equation for the analytical values can be easily derived or found in most multiphase flows text book (see Hu [22]). For the 53 mm pipe [21], the present results are slightly higher than those from the laminar analytical solution. However, the present results are significantly lower than the experimental values for a bulk velocity, *U* greater than 1.5 m/s. Meanwhile, for the 158 mm pipe [1], the present results are more in good agreement with experimental data than the laminar analytical values (Fig. 6). The stress ratio ($\tau_y$ / $\tau_w$) or plug region values range from approximately 0.32 to 0.61 and 0.63 to 0.74, respectively, for 53 mm and 158 mm pipe diameters. Therefore, it is tempting to ascribe the performance to the change in velocity profile although GTM developers [14-16] seem to somehow address it empirically. It has been observed experimentally for Herschel-Bulkley fluids that, both laminar and turbulent flow conditions exist in the fully developed region [23-25]. In addition, Peixinho et al [22] found that in the early stages of the transition regime, the near-wall region is turbulent whereas the core region is laminar. Therefore, the relaminarization in the fully developed region (see Fig. 7) does not seem to be capturing the local flow phenomenon, and thereby under-predicting the pressure drop, especially for low stress ratio values. It is worth mentioning that, although not shown here the same observation was made for Newtonian fluid.

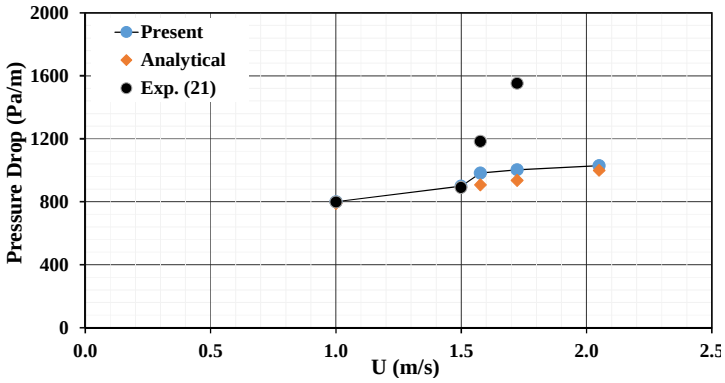


**Figure 5**: Comparison of the pressure drop in 53 mm pipe diameter

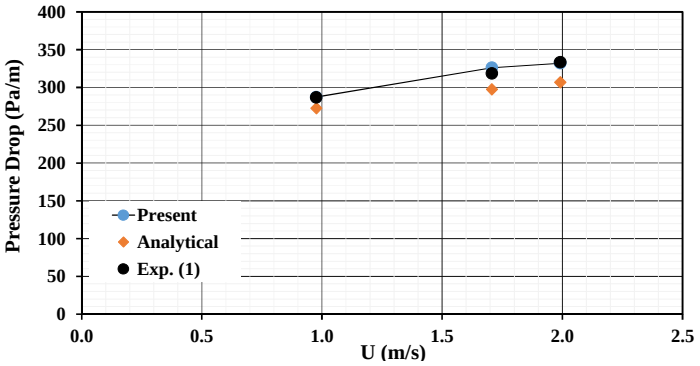


**Figure 6**: Comparison of the pressure drop in 158 mm pipe diameter

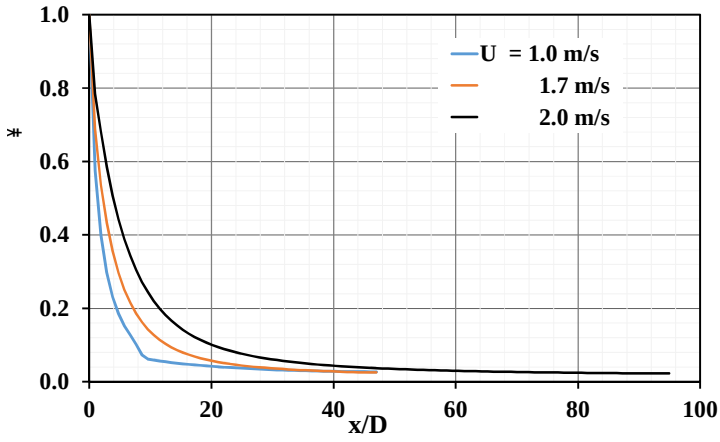


**Figure 7**: Turbulent intermittency along the streamwise direction at y/D = 0.1 in 158 mm pipe diameter

## CONCLUSION

Selected empirical or semi-empirical engineering models were used to predict transition velocity of non-Newtonian slurry flows in a horizontal pipe. Several datasets from different pipe diameters (25 – 268 mm) were used. Using the last laminar data point as the transition velocity, it was found that the prediction of most models is somewhat conservative. However, caution should be exercised in design situations where both the pipe diameter and viscoplastic viscosity influence the value of the Hedström number. In general, the notion that at higher pipe diameters ($He > 1.0 \times 10^5$), transition velocity is only a function of the yield stress and slurry density might have to be revisited. The model by Wilson and Thomas [3] seems to give better predictions of the data used in the present work.

For low stress ratio ($\tau_y / \tau_w$), GTM in ANSYS CFX gave pressure drops similar to the analytical laminar flow condition and lower than those from experimental transition conditions. An excellent agreement between GTM and experimental transition conditions was observed for higher stress ratios. However, streamwise turbulent intermittency values suggested relaminarization in the fully developed region indicating the effect of the change of velocity profile. In addition, since for viscoplastic fluids, the flow core is very viscous recalibration of the empirical correlation maybe required. Finally, the GTM fails to capture some of the experimentally observed local flow phenomenon.

## NOMENCLATURE

| | |
|---|---|
| $D$ | pipe diameter (m) |
| $F_{length}$ | length of the transition zone (-) |
| He | Hedström number (-) |
| $k$ | turbulent kinetic energy ($m^2/s^2$) |
| Re | Reynolds number (-) |
| $Re^{-}_{c}$ | Reynolds number (-) |
| $Re^{-}_{t}$ | Reynolds number (-) |
| $U$ | bulk velocity (m/s) |
| $u$ | local velocity (m/s) |
| $V_T$ | transitional velocity (m/s) |
| $x$ | streamwise direction coordinate (m) |
| $y$ | transverse direction coordinate (m) |
| $y_n$ | wall normal distance (m) |
| $z$ | spanwise direction coordinate (m) |

*Greek*

| | |
|---|---|
| µ | specific dissipation rate ($s^{-1}$) |
| t | absolute value of the strain rate ($s^{-1}$) |
| ¥ | turbulent intermittency (-) |
| $^2_w$ | wall shear stress (Pa) |
| $^2_y$ | yield stress (Pa) |
| $\rho$ | density ($kg/m^3$) |
| « | apparent viscosity (Pa·s) |
| $«_p$ | Bingham plastic viscosity ratio (Pa·s) |
| $«_t$ | Eddy viscosity ratio (Pa·s) |

## ACKNOWLEDGMENTS

The support from FastCFD Solutions Inc. and its clients is gratefully acknowledged.

## REFERENCES


1. Xu, J., Gillies, R., Small, M., and Shook, C., 1993, "Laminar and Turbulent Flow of Kaolin Slurries", *Hydrotransport*, 12, 595-613.
2. Slatter, P. T. and Wasp, E. J., 2000. "The Laminar-Turbulent Transition in Large pipes", Proceedings of the *10th International Conference on Transport and Sedimentation of Solid Particles*, Wroclaw, 4-7 September 2000, 389-399.
3. Wilson, K. C. and Thomas, A. D., 2006 "Analytic Model of Laminar-Turbulent Transition for Bingham Plastics", *The Canadian Journal of Chemical Engineering*, **84**(5), 520-526.
4. Van den Heever, E., 2013, "Rheological Model Influence on Pipe Flow Predictions for Homogeneous non-Newtonian Fluids", *Masters Thesis, Department of Civil Engineering*, Cape Peninsula University of Technology, Cape Town, South Africa.
5. Malin, M. R., 1997, "The Turbulent Flow of Bingham Plastic Fluids in Smooth Circular Pipes," *Intentional Journal of Heat Mass Transfer*, (6), 793–804.
6. Güzel, B., Frigaard, I., and Martinez, D. M., 2009, "Predicting Laminar–Turbulent Transition in Poiseuille Pipe Flow for Non-Newtonian Fluids, *Chemical Engineering Science*, **64** (2), 254-264.
7. Sutherland, A., Haldenwang, R., Chhabra, R., and van den Heever, E., 2015. "Selecting the best Rheological and Pipe Turbulent Flow Prediction Models for non-Newtonian Fluids-Use of RMSE and $R^2$ vs. AIC", Proceedings of the *17th International Conference on Transport and Sedimentation of Solid Particles*, Delft, 22-25 September 2015, 317-326.
8. Liu, W-J., Burgess, K., Roudnev, A., and Bootle, M., 2009, "Pumping non-Newtonian Slurries", *Technical Bulletin*, Weir Minerals Division, **14** (2), 1-4.
9. Swamee, P. K. and Aggarwal, N., 2011, "Explicit Equations for Laminar Flow of Bingham Plastic Fluids," *Journal of Petroleum Science and Engineering*, **76** (3–4), 178-184.
10. Hedström, B. O. A., 1952, "Flow of Plastics Materials in Pipes," *Industrial Engineering Chemistry*, **44**(3), 651–656.
11. Shook, C. A. and Roco, M. C., 1991, "Slurry Flow: Principles and Practice", Boston: Butterworth-Heinemann.
12. Menter, F. R., 1994, "Two-equation Eddy-viscosity Turbulence Models for Engineering Applications", *AIAA-Journal*, **32**, 1598 - 1605.
13. Wilcox, D. C., 1988, "Multiscale Model for Turbulent Flows", *AIAA-Journal*, **26**, 1311-1320.
14. Menter, F. R., Langtry, R. B., Likki, S.R., Suzen, Y. B., Huang, P. G., and Völker, S., 2004, "A Correlation based Transition Model using Local Variables Part 1- Model Formulation", ASME-GT2004-53452, *ASME TURBO EXPO 2004*, Vienna, Austria.
15. Langtry, R. B., Menter, F. R., Likki, S. R., Suzen, Y. B., Huang, P. G., and Völker, S., 2004, "A Correlation based Transition Model using Local Variables Part 2 - Test Cases and Industrial Applications", ASME-GT2004-53454, *ASME TURBO EXPO 2004*, Vienna, Austria.
16. Langtry, R. B. and Menter, F. R., 2005, "Transition Modeling for General CFD Applications in Aeronautics", AIAA paper 2005-522.
17. Adane, K. F. K., Shah, S. I. A., and Sanders, R. S., 2012, "Numerical Study of Liquid-Liquid Vertical Dispersed Flows", *ASME 2012 Fluids Engineering Summer Meeting*, 1651-1658, Rio Grande, Puerto Rico, July 8-12, 2012.
18. Antaya, C. L., Adane, K. F. K. and Sanders, R. S., 2012, "Modelling Concentrated Slurry Pipeline Flows", *ASME 2012 Fluids Engineering Summer Meeting*, 1659-1671, Rio Grande, Puerto Rico, July 8-12, 2012.
19. Hashemi, S. A., Spelay, R. B., Adane, K. F. K., and Sanders, R. S., 2014, "Solids Velocity Fluctuations in Concentrated Slurries", Hydrotransport 19, Edited by R. S. Sanders and R. Sumner, Golden, CO, USA, 24-26 September 2014, 391-403.
20. Litzenberger, C. G., 2003, "Rheological Study of Kaolin Clay Slurries", *Masters Thesis, Department of Chemical Engineering*, University of Saskatchewan, Saskatoon, Canada.
21. Spelay, R. B., 2007, "Solids Transport in Laminar, Open Channel Flow of Non-Newtonian Slurries", *PhD Thesis, Department of Chemical Engineering*, University of Saskatchewan, Saskatoon, Canada.
22. Hu, S., 2006, "Slurry Flows", Chapter 4, *Multiphase Flow Handbook*, ed. Crowe, C.T., CRC press, 59, 4-50-60.
23. Peixinho, J., Nouar, C., Desaubry, C., Théron, B., 2005, "Laminar Transitional and Turbulent Flow of Yield Stress Fluid in a Pipe", *Journal of Non-Newtonian Fluid Mechanics*, **128** (2–3), 172-184.
24. Rudman, M., Graham, L. J., Blackburn, H. M., Pullum, L., 2002, "Non-Newtonian Turbulent and Transitional Pipe Flow", *Hydrotransport 15*, Banff, Canada.
25. Esmael, A. and Nouar, C., 2008, "Transitional Flow of a Yield-stress Fluid in a Pipe: Evidence of a Robust Coherent Structure", *Physical Review E*, **77** (5): 057302.